J Intell Robot Syst (2014) 75:595–608
DOI 10.1007/s10846-013-9838-2

Robust Tracking Control of a Quadrotor Helicopter

Hao Liu · Yongqiang Bai · Geng Lu · Zongying Shi · Yisheng Zhong

Received: 3 September 2012 / Accepted: 26 April 2013 / Published online: 11 May 2013

Abstract In this paper, a robust tracking control method for automatic take-off, trajectory tracking, and landing of a quadrotor helicopter is presented. The designed controller includes two parts: a position controller and an attitude controller. The position controller is designed by the static feedback control method to track the desired trajectory of the altitude and produce the desired angles for pitch and roll angles. By combining the proportional-derivative (PD) control method and the robust compensating technique, the attitude controller is designed to track the desired pitch and roll angles and stabilize the yaw angle. It is proven that the attitude tracking error of each channel can converge to the given neighborhood of the origin ultimately. Experimental results demonstrate the effectiveness of the designed control method.

H. Liu (✉) · G. Lu · Z. Shi · Y. Zhong
Department of Automation, TNList,
Tsinghua University, Beijing, 100084,
People's Republic of China
e-mail: liuhao08@mails.tsinghua.edu.cn

Y. Bai
Luoyang Electronic Equipment Test Center of China,
Henan Province, Luoyang 471003,
People's Republic of China

Keywords Quadrotor helicopter · Robust control · Trajectory tracking · Automatic take-off and landing

1 Introduction

In the last decade, unmanned helicopters have attracted much attention due to their various applications such as search, rescue, surveillance, interdiction, and transportation. Intensive research efforts have been devoted to quadrotor helicopters because of their advantages over the conventional helicopters: the quadrotors have more compact structures with four smaller efficient rotors; the attitude angles can be controlled by varying the angular speeds of the rotors without swashplates; tail rotors are not needed to compensate the torques produced by main rotors in conventional helicopters (see, also in [1, 2]).

The unmanned helicopter is one of the most complex systems and its dynamics involves nonlinearity, uncertainties, and coupling (see, e.g., [3–6]). Many works have been done on the controller design for the quadrotor helicopter. PD^2 feedback control method was employed to stabilize the attitude of a quadrotor aircraft in [7]. By combining model predictive control strategy and nonlinear H_∞ control approach, Raffo et al. [8] discussed the path following problem. In [9], a station-keeping and tracking controller was

designed to deal with underactuation and strong coupling in pitch-yaw-roll. In [10], the singular perturbation theory was used to design a hierarchical controller for a miniature helicopter. Precision hovering and trajectory tracking were achieved for a multi-vehicle quadrotor helicopter as shown in [11].

Previous experimental results mainly focused on the hovering control or trajectory tracking control problems for quadrotor helicopters (see, e.g., [1–4, 7, 10, 11]). Research on the automatic take-off and landing problems for this kind of helicopter remains challenging because of the ground effect that the helicopter is subject to. The lift thrusts produced by the rotor blades will change when the helicopter flies near the ground. Nonlinear feedback controllers were applied for a scale model helicopter and a conventional helicopter to achieve the take-off flight and the automatic landing in [12] and [13], respectively. But, the effects of uncertainty existing in the take-off and landing control were not fully discussed in their papers.

One of the solutions to improving controller performances in take-off and landing tasks is to design a controller which is robust against these disturbances. In this paper, a robust controller is designed by the time-scale separation approach with two parts: a position controller and an attitude controller. In order to achieve the motion control of the quadrotor, the position controller is applied to generate the desired pitch and roll angles from the information of the position tracking errors and track the desired altitude reference. Furthermore, by combining the proportional-derivative (PD) control method and the robust compensating technique, an attitude controller is designed to track the desired attitude angles. The parameters of the attitude controller are firstly tuned: one can tune the PD controller parameters in hovering condition without the robust compensator; then, the robust compensator parameters can be tuned on-line. The parameters of the position controller are tuned for position control tasks after the attitude controller parameters are determined in hovering flight. It is proven that the attitude tracking error of each channel is ultimately bounded with specified boundary. Our previous studies focused on the robust control problem of a reduced-order three degree-of-freedom (3-DOF) helicopter (see, for example, [14–16]). However, the quadrotor helicopter has 6-DOF and contains serious coupling between the angular velocities and the angles in the rotational dynamics. Furthermore, in this paper, the inequalities of the bounds of the disturbances involve the quadratic terms of the state in the stability analysis and the tracking performance of the closed-loop system can be guaranteed for large-angle tracking missions.

The following parts of this paper are laid out as follows. Dynamical model of the quadrotor aircraft is presented in Section 2. Section 3 describes the robust controller design procedure. In Section 4, the robust properties of the closed-loop system are proven. Experimental results on the quadrotor aircraft are given in Section 5 and conclusion remarks are drawn in Section 6.

Notations For $y(t) = [y_i(t)] \in L_\infty^n$ and $h(t) = [h_{ij}(t)] \in L_1^{m\times n}$, define that

$$\|y\|_\infty = \max_i \sup_{t\geq 0} |y_i(t)|\,, \|H(p)\|_1 = \|h\|_1 = \max_i \left(\sum_j \int_0^\infty |h_{ij}(t)|\, dt \right)$$

where p is the Laplace operator, $H(p) = \ell(h(t))$, and $\ell(\cdot)$ indicates the Laplace transform.

2 Control Problem Statement

2.1 System Description

The Tsinghua Autonomous Quadrotor System (TAQS), as depicted in Fig. 1, is developed as a platform to examine the effectiveness of newly developed linear or nonlinear control method. It is based on the mechanical frame of the X-aircraft X650, which is a remote-control aircraft for commercial aerial photography. The avionic electronic system includes an onboard flight control computer, a sensor system, and four high speed brushless DC speed controllers. A DSP, TMS320F28335, is used as a flight control computer to implement the control algorithms. The sensor system consists of an inertial measurement

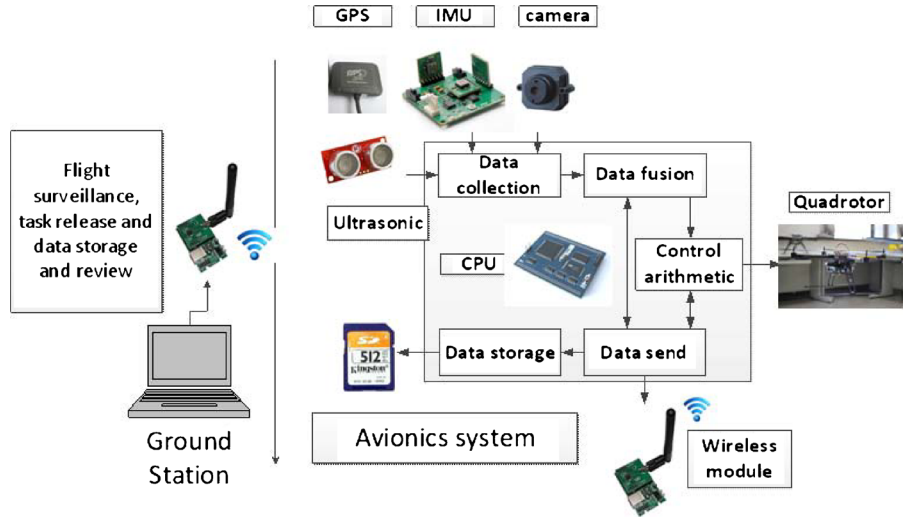

Fig. 1 The Tsinghua Autonomous Quadrotor System

unit (IMU) module (which includes a 3-axis digital output linear accelerometer, three gyroscopes, and a compass), a sonar sensor, and an onboard camera. The onboard camera is used for obtaining the position information and the sonar is applied to measure the altitude in indoor environments. A ground station receives flight data from the DSP by a pair of the Zigbee wireless.

2.2 Dynamical Model of the Quadrotor Helicopter

As shown in Fig. 2, the four-rotor helicopter has 6-DOF: three translational components and three rotational components, and has four control inputs: four thrusts produced by the four rotors. The four rotors are divided into two pairs (1, 3) and (2, 4), where rotors (1, 3) rotate clockwise and rotors (2, 4) rotate clockwise. Increasing or decreasing the sum of the thrusts results in the vertical motion. The pitch movement is obtained by changing the thrust of rotor (1) while altering the thrust of rotor (3) conversely. Similarly using the rotors (2, 4) can result in the roll movement. The yaw movement results from the difference between the reactive torques produced by rotors (1, 3) and (2, 4). An offset in the roll or pitch angle leads to the lateral or longitudinal motion. In this section, the model of the six motions of the quadrotor helicopter corresponding to the four inputs will be discussed.

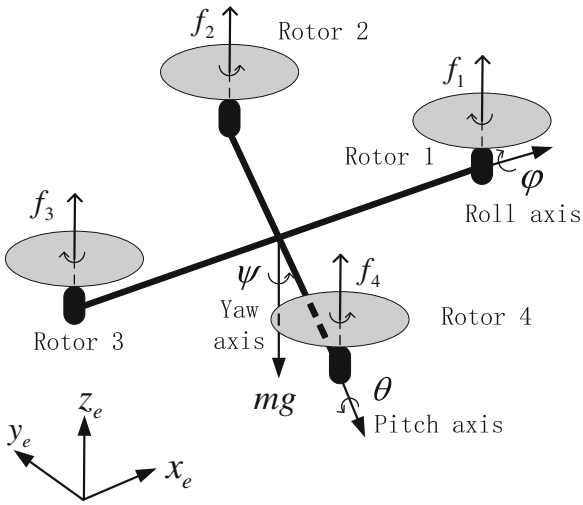

Fig. 2 The schematic of the quadrotor helicopter

Let $E = \{x_e, y_e, z_e\}$ indicate the earth-fixed initial frame and $B = \{x_b, y_b, z_b\}$ the frame rigidly attached to the rotorcraft body as shown in Fig. 2. The Euler angles $\eta = [\varphi\ \theta\ \psi]^T$, representing the roll, pitch, and yaw angles respectively, determine the orientation matrix R from B to E as

$$R = \begin{bmatrix} C_\theta C_\psi & C_\psi S_\varphi S_\theta - C_\varphi S_\psi & S_\varphi S_\psi + C_\varphi C_\psi S_\theta \\ C_\theta S_\psi & C_\varphi C_\psi + S_\varphi S_\theta S_\psi & C_\varphi S_\theta S_\psi - C_\psi S_\varphi \\ -S_\theta & C_\theta S_\varphi & C_\varphi C_\theta \end{bmatrix},$$

where $C_\bullet = \cos(\cdot)$ and $S_\bullet = \sin(\cdot)$. Let $\xi = [\xi_x\ \xi_y\ \xi_z]^T$ denote the position of the center of the mass of the rotorcraft in the frame E, where ξ_x, ξ_y, and ξ_z indicate the longitude, lateral, and height positions respectively. The helicopter

motion equations can be obtained according to Newton's law as

$$F = m\ddot{\xi},$$
$$\tau = \frac{dH}{dt},$$

where F is the external force acting on the quadrotor helicopter, τ the external torque of the helicopter, H the angular momentum of the rotorcraft relative to the inertial frame E, and m the mass of the quadrotor. The helicopter motion equations, shown in the above equations, can be rewritten as follows (see, also [3])

$$\begin{aligned}
\ddot{\xi}_x &= f(\cos\varphi\sin\theta\cos\psi + \sin\varphi\sin\psi)/m,\\
\ddot{\xi}_y &= -f(\sin\varphi\cos\psi - \cos\varphi\sin\theta\sin\psi)/m,\\
\ddot{\xi}_z &= f\cos\varphi\cos\theta/m - g,\\
\ddot{\varphi} &= -c_\varphi(\eta,\dot{\eta})\dot{\eta} + a_{\varphi 1}\tau_\varphi,\\
\ddot{\theta} &= -c_\theta(\eta,\dot{\eta})\dot{\eta} + a_{\theta 1}\tau_\theta,\\
\ddot{\psi} &= -c_\psi(\eta,\dot{\eta})\dot{\eta} + a_{\psi 1}\tau_\psi,
\end{aligned} \tag{1}$$

where g is the gravity constant, f the sum of the four thrusts, $a_{i1}(i = \varphi, \theta, \phi)$ helicopter parameters determined by the time-domain based system identification approach, $\tau = \left[\tau_\phi\ \tau_\theta\ \tau_\psi\right]^T$ the external body-fixed frame torques about the pitch, roll, and yaw angles respectively, and $c_i(\eta,\dot{\eta})(i = \varphi, \theta, \phi)$ the Coriolis terms. The Coriolis terms include the gyroscopic and centrifugal terms as shown in [3]. The details of the expressions of the Coriolis terms are depicted in [8], and one can see that there exist positive constants $\xi_{\eta i}$ and $\xi_{\dot{\eta} i}(i = \varphi, \theta, \phi)$ satisfy that $\|c_i(\eta,\dot{\eta})\|_\infty \le \xi_{\eta i}\|\eta\|_\infty + \xi_{\dot{\eta} i}\|\dot{\eta}\|_\infty (i = \varphi, \theta, \phi)$. τ and f are determined by

$$\tau_\phi = l_f(f_2 - f_4),\ \tau_\theta = l_f(f_1 - f_3),$$
$$\tau_\psi = k_f(f_1 - f_2 + f_3 - f_4),\ f = f_1 + f_2 + f_3 + f_4,$$

where l_f is the distance from each motor to the center of the mass, $k_f > 0$ denotes the force-to-moment scaling factor, and $f_i(i = 1, 2, 3, 4)$ are the thrusts produced by the four rotors respectively. Let $b_\varphi = a_{\varphi 1} l_f$, $b_\theta = a_{\theta 1} l_f$, and $b_\psi = a_{\psi 1} k_f$. Define the control inputs $u_i(i = 1, 2, 3, 4)$ as

$$u_1 = f_2 - f_4,\ u_2 = f_1 - f_3,\ u_3 = f_1 - f_2 + f_3 - f_4,\ u_4 = f.$$

Assumption 1 The uncertain parameters $a_i(i = \varphi, \theta, \phi)$ and $b_i(i = \varphi, \theta, \phi)$ are bounded. Their nominal parameters $b_i^N(i = \varphi, \theta, \phi)$ are positive and satisfy that $\left|b_i^N - b_i\right| < b_i^N$.

Define $\rho_1 = \left|b_\varphi^N - b_\varphi\right|/b_\varphi^N$, $\rho_2 = \left|b_\theta^N - b_\theta\right|/b_\theta^N$, and $\rho_3 = \left|b_\psi^N - b_\psi\right|/b_\psi^N$.

Remark 1 If the Assumption 1 holds, one can obtain that $\rho_i < 1(i = 1, 2, 3)$.

Assumption 2 The roll and pitch angles satisfy that $\varphi \in [-\pi/2 + \delta_\varphi, \pi/2 - \delta_\varphi]$ and $\theta \in [-\pi/2 + \delta_\theta, \pi/2 - \delta_\theta]$ with δ_φ and δ_θ positive constants.

Remark 2 The rotorcraft is required to avoid overturning during the flight in order to avoid singularities in the Euler angle representation [17].

Assumption 3 The sum f of the thrusts is bounded and satisfy that $f \ge \delta_f$, where δ_f is a positive constant.

Remark 3 If descent maneuvers are never faster than a free fall condition, one can obtain that sum of the thrusts is strictly positive [18].

In this article, the three positions and the yaw angle $\{\xi_x, \xi_y, \xi_z, \psi\}$ are chosen as the outputs and their prescribed reference signals are denoted as $i_d(i = x, \mathrm{y}, \mathrm{z}, \psi)$ respectively.

Assumption 4 The prescribed reference signals and their derivatives $i_d^{(k)}(i = x, \mathrm{y}, \mathrm{z}, \psi;\ k = 0, 1, 2)$ are piecewise uniformly bounded.

3 Robust Controller Design

A classical method to design the motion controller for aircrafts is based on the time-scale separation approach. This approach replies on the assumption that the closed-loop attitude dynamics can

converge much faster than the closed-loop translational dynamics by applying, e.g., a high-gain attitude controller [10]. Thus, the whole closed-loop system can be stabilized in practical applications. In this section, a motion controller, consisting a position controller and a high-gain robust attitude controller, will be discussed.

Quadrotor helicopter model (1) can be rewritten as

$$\begin{aligned}
\ddot{\xi}_x &= f(\cos\varphi\sin\theta\cos\psi+\sin\varphi\sin\psi)/m,\\
\ddot{\xi}_y &= -f(\sin\varphi\cos\psi-\cos\varphi\sin\theta\sin\psi)/m,\\
\ddot{\xi}_z &= u_4\cos\varphi\cos\theta/m-g,\\
\ddot{\varphi} &= b_\varphi^N u_1+q_1,\\
\ddot{\theta} &= b_\theta^N u_2+q_2,\\
\ddot{\psi} &= b_\psi^N u_3+q_3,
\end{aligned}\tag{2}$$

where $q_i(i=1,2,3)$ are the named equivalent disturbances and take the following forms

$$\begin{aligned}
q_1 &= (b_\varphi - b_\varphi^N)u_1 - c_\varphi(\eta,\dot{\eta})\dot{\eta},\\
q_2 &= (b_\theta - b_\theta^N)u_2 - c_\theta(\eta,\dot{\eta})\dot{\eta},\\
q_3 &= (b_\psi - b_\psi^N)u_3 - c_\psi(\eta,\dot{\eta})\dot{\eta}.
\end{aligned}\tag{3}$$

From Eq. 2, one can see that the robust tracking control in the longitudinal and lateral directions can be achieve by controlling the attitude angles θ and φ appropriately, if the three positions and the yaw angle are chosen as the outputs. The position controller designed in this section will produce the desired attitude signals θ_d and φ_d for θ and φ to track based on the tracking errors of the longitudinal and lateral positions ξ_x and ξ_y, respectively; the position controller will also be used to track the height reference z_d for the position ξ_z. The attitude controller will be applied to track the references signals θ_d, φ_d, and ψ_d for the three attitude angles.

3.1 Position Controller Design

The position controller generates the desired references for the pitch and roll angles and stabilizes the height of the quadrotor.

Define the saturation function $sat_c(d) = \mathrm{sgn}(d)\min\{|d|, c\}$ with c a positive constant. Then, design position feedback control laws in the longitudinal and lateral directions based on the static feedback control method as

$$\begin{aligned}
\theta_d &= -\arcsin sat_{1-c_{\mathrm{sat}}}\left(\frac{mk_x^p(\xi_x-x_d)+mk_x^d\left(\dot{\xi}_x-\dot{x}_d\right)-m\ddot{x}_d+f\sin\varphi\sin\psi}{f\cos\varphi\cos\psi}\right),\\
\varphi_d &= \arcsin sat_{1-c_{\mathrm{sat}}}\left(\frac{mk_y^p(\xi_y-y_d)+mk_y^d\left(\dot{\xi}_y-\dot{y}_d\right)-m\ddot{y}_d+f\cos\varphi\sin\theta\sin\psi}{f\cos\psi}\right),
\end{aligned}\tag{4}$$

where k_i^p and $k_i^d(i=x,y)$ are positive parameters to be determined and c_{sat} is a positive constant satisfying $c_{\mathrm{sat}}<1$.

Furthermore, the static feedback controller for the vertical channel can be designed as

$$\begin{aligned}
u_4 = \big(&-k_z^p(\xi_z-z_d)-k_z^d\left(\dot{\xi}_z-\dot{z}_d\right)+\ddot{z}_d\\
&+mg\big)/\cos\varphi/\cos\theta,
\end{aligned}\tag{5}$$

with positive parameters k_z^p and k_z^d to be determined.

If the closed-loop attitude dynamics can converge much faster than the closed-loop translational dynamics, one can expect that $\theta=\theta_d$ and $\varphi=\varphi_d$ when the translational dynamics is considered. In this case, the position static feedback control laws (4) are designed to guarantee that the closed-loop translational systems of the longitudinal and lateral channels have the following forms by ignoring saturation functions

$$\left(\ddot{\xi}_i-\ddot{i}_d\right)+k_i^d\left(\dot{\xi}_i-\dot{i}_d\right)+k_i^p(\xi_i-i_d)=0(i=x,y).\tag{6}$$

Similarly, from Eqs. 2 and 5, one has that

$$\left(\ddot{\xi}_z-\ddot{z}_d\right)+k_z^d\left(\dot{\xi}_z-\dot{z}_d\right)+k_z^p(\xi_z-z_d)=0.$$

The stability of the closed-loop translational systems can be guaranteed by selecting proper parameters k_i^p and $k_i^d(i=x,y,z)$ so that the roots of

the polynomial $p^2 + k_i^d p + k_i^p = 0$ are all negative constants.

3.2 Attitude Controller Design

In this subsection, a robust high-gain attitude controller will be designed to follow the references signals θ_d, φ_d, and ψ_d for the three attitude angles.

Define $u = \left[u_1 \; u_2 \; u_3 \right]^T$. The control input u consists of two parts: the PD control input u^{PD}, and the signal compensating input u^{SC}; that is, the control input can be expressed as

$$u = u^{PD} + u^{SC}. \tag{7}$$

The elements of u have the corresponding two parts: $u_i = u_i^{PD} + u_i^{SC} (i = 1, 2, 3)$. Furthermore, define $q = \left[q_1 \; q_2 \; q_3 \right]^T$ and $x = [x_i]_{6\times 1}$, where $x_1 = \varphi - \varphi_d$, $x_2 = \theta - \theta_d$, $x_3 = \psi - \psi_d$, and $x_{i+3} = \dot{x}_i (i = 1, 2, 3)$. Then, one can have that

$$\dot{x} = Ax + B(u + \Delta). \tag{8}$$

where $\Delta = \left[(q_1 - \ddot{\varphi}_d)/b_\varphi^N (q_2 - \ddot{\theta}_d)/b_\theta^N (q_3 - \ddot{\psi}_d)/b_\psi^N \right]^T$, and

$$A = \begin{bmatrix} 0\,0\,0\,1\,0\,0 \\ 0\,0\,0\,0\,1\,0 \\ 0\,0\,0\,0\,0\,1 \\ 0\,0\,0\,0\,0\,0 \\ 0\,0\,0\,0\,0\,0 \\ 0\,0\,0\,0\,0\,0 \end{bmatrix}, \; B = \begin{bmatrix} 0 & 0 & 0 \\ 0 & 0 & 0 \\ 0 & 0 & 0 \\ b_\varphi^N & 0 & 0 \\ 0 & b_\theta^N & 0 \\ 0 & 0 & b_\psi^N \end{bmatrix}.$$

The PD controller is constructed as

$$u_i^{PD} = -k_i^p x_i - k_i^d x_{i+3} (i = 1, 2, 3). \tag{9}$$

where k_i^p and $k_i^d (i = 1, 2, 3)$ are Positive constants.

Define

$$\mathrm{K} = \begin{bmatrix} k_1^p & 0 & 0 & k_1^p & 0 & 0 \\ 0 & k_2^p & 0 & 0 & k_2^d & 0 \\ 0 & 0 & k_3^p & 0 & 0 & k_3^d \end{bmatrix}.$$

The PD controller parameters k_i^p and $k_i^d (i = 1, 2, 3)$ are selected such that $A_H = A - BK$ is Hurwitz.

Remark 4 In practical applications, the position controller parameters k_i^p and $k_i^d (i = x, y, z)$ and the PD attitude controller parameters k_j^p and $k_j^d (j = 1, 2, 3)$ can be determined by the pole placement method.

From Eqs. 7, 8, and 9, one can obtain that

$$\dot{x} = A_H x + B\left(u^{SC} + \Delta\right). \tag{10}$$

The signal compensating input u^{SC} is designed as follows in order to restrain the influences of the uncertainty Δ (see also in [14–16, 19])

$$u^{SC}(p) = -F(p)\Delta(p), \tag{11}$$

where $F_i(p) = diag(F_1(p), F_2(p), F_3(p))$, $F_i(p) = g_{i1}g_{i2}/(p^2 + g_{i1}p + g_{i2}p + g_{i1}g_{i2})$ $(i = 1, 2, 3)$ with parameters g_{i1} and g_{i2} to be determined. If the parameters g_{i1} and $g_{i2} (i = 1, 2, 3)$ are sufficiently large and satisfy $g_{i1} \gg g_{i2} > 0 (i = 1, 2, 3)$, one can expect that the robust filters $F_i(p) (i = 1, 2, 3)$ would have sufficiently wide frequency bandwidths and within them the filter gains would approximate 1. However, uncertainties $\Delta(p)$ in Eq. 11 cannot be obtained in practical applications. Therefore, one has to obtain the expressions of the control inputs $u^{SC}(p)$ which does not depend on $\Delta(p)$. From Eqs. 8 and 11, the robust compensator can be realized with states z_{i1} and $z_{i2} (i = 1, 2, 3)$ as follows

$$\begin{aligned} \dot{z}_{i1} &= -g_{i2} z_{i1} - g_{i2}^2 x_i + b_i^N u_i, \\ \dot{z}_{i2} &= -g_{i1} z_{i2} + (g_{i1} + g_{i2}) x_i + z_{i1}, \\ u_i^{SC} &= g_{i1} g_{i2} (z_{i2} - x_i)/b_i^N, \; i = 1, 2, 3. \end{aligned} \tag{12}$$

The whole configuration of the robust control strategy is depicted in Fig. 3.

4 Robust Properties Analysis

This section will prove the robust attitude tracking properties of the closed-loop system consisting of Eqs. 2, 7, 9, and 12.

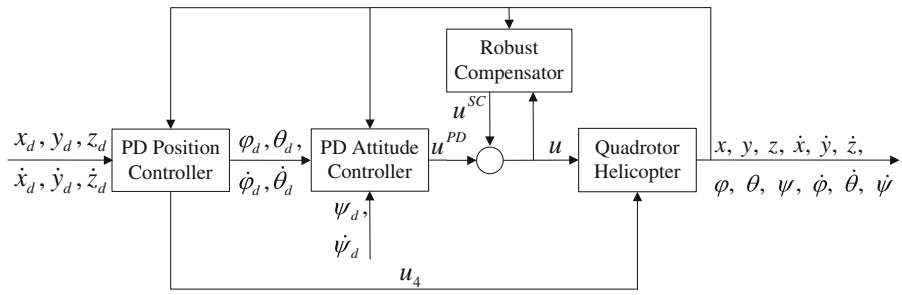

Fig. 3 The block diagram of the robust control system

Theorem 1 *If Assumptions* 1 *through* 4 *hold, for the given initial state* $x(0)$ *and the given positive constant* ε*, there exist positive constants* g_1^**,* g_2^**, and* T^**, such that if* $g_{i1} \geq g_1^*$*,* $g_{i2} \geq g_2^*$*, and* $g_{i1} \gg g_{i2} (i = 1, 2, 3)$*, then the state* $x(t)$ *are bounded and satisfies* $\max_i |x_i(t)| \leq \varepsilon, \forall t \geq T^*$.

Proof Combining (10) and (11), one can obtain that

$$\|x\|_\infty \leq \mu_{x(0)} + \left\|(pI_{6\times 6} - A_H)^{-1} B(I_{3\times 3} - F)\right\|_1 \|\Delta\|_\infty, \quad (13)$$

where $I_{n\times n}$ is an $n \times n$ unit matrix, and $\mu_{x(0)} = \max_i \sup_{t\geq 0} \left|e_i^T e^{A_H t} x(0)\right|$, where e_i is a 6×1 vector with one on the ith row and zeros elsewhere. Define $\gamma = \left\|(pI_{6\times 6} - A_H)^{-1} B(I_{3\times 3} - F)\right\|_1$. Then from [15], one can obtain that if g_{i1} and $g_{i2} (i = 1, 2, 3)$ are sufficiently large and satisfying that $g_{i1} \gg g_{i2} > 0$, γ can be made as small as desired and there exists a positive constant μ_γ satisfying $\gamma < \mu_\gamma / \min_i\{g_{i2}\}$.

If the attitude reference signals and their derivatives $i_d^{(k)} (i = \varphi, \theta, \psi;\ k = 0, 1, 2)$ are piecewise uniformly bounded, then from Eqs. 3, 6, 8, and 10, there exist positive constants μ_x, μ_{x2}, and μ_c such that

$$\|\Delta\|_\infty \leq \mu_x \|x\|_\infty + \mu_{x2} \|x\|_\infty^2 + \mu_c. \quad (14)$$

If x satisfies that

$$(\mu_x + \mu_{x2} \|x\|_\infty)(\sqrt{\gamma} + \gamma) \leq 1, \quad (15)$$

one can obtain the following equation

$$\|\Delta\|_\infty \leq (\mu_{x(0)} + \mu_c/\mu_x)/\sqrt{\gamma}. \quad (16)$$

From Eqs. 13 and 16, one has that

$$\|x\|_\infty \leq \mu_{x(0)} + \sqrt{\gamma}(\mu_{x(0)} + \mu_c/\mu_x).$$

Then one can see that $\|x\|_\infty$ is bounded.

From Eq. 15, one can have the attractive region as

$$\left\{x : \|x\|_\infty \leq \mu_{x2}^{-1}/(\sqrt{\gamma} + \gamma) - \mu_{x2}^{-1}\mu_x\right\}. \quad (17)$$

Fig. 4 The TAQS in hover

Table 1 Helicopter parameters

Helicopter parameter	Value	Helicopter parameter	Value
m	1.6	b_φ^N	9.207
b_θ^N	9.700	b_ψ^N	15.988

Thus, if $x(t)$ starts from the attractive region and γ is sufficiently small so that

$$\mu_{x(0)} + (\mu_{x(0)} + \mu_c/\mu_x)\sqrt{\gamma} \le \mu_{x2}^{-1}/\left(\sqrt{\gamma} + \gamma\right) - \mu_{x2}^{-1}\mu_x, \tag{18}$$

then $x(t)$ can remain inside the attractive region. It follows that if Eq. 18 holds and the initial state $x(0)$ satisfies

$$\|x(0)\|_\infty < \mu_{x2}^{-1}/\left(\sqrt{\gamma} + \gamma\right) - \mu_{x2}^{-1}\mu_x, \tag{19}$$

one can obtain (15).

From Eqs. 10, 11, and 16, one has that

$$\max_i |x_i(t)| \le \max_i \left|e_i^T e^{A_\mu t} x(0)\right| + \sqrt{\gamma}\left(\mu_{x(0)} + \mu_c/\mu_x\right). \tag{20}$$

Therefore if γ is chosen to satisfy that $\gamma < \varepsilon^2/(\mu_{x(0)} + \mu_c/\mu_x)^2/4$, then one can obtain a positive constant T^* and sufficiently large positive parameters g_1^* and g_2^*, such that if $g_{i1} \ge g_1^*$, $g_{i2} \ge g_2^*$, and $g_{i1} \gg g_{i2}(i = 1, 2, 3)$, one has that $\max_i |x_i(t)| \le \varepsilon, \forall t \ge T^*$. □

Remark 5 Theoretically, the robust compensator parameters g_{i1} and $g_{i2}(i = 1, 2, 3)$ are chosen satisfying that $g_{i1} \gg g_{i2}(i = 1, 2, 3)$ and $\min_i\{g_{i2}\} >$

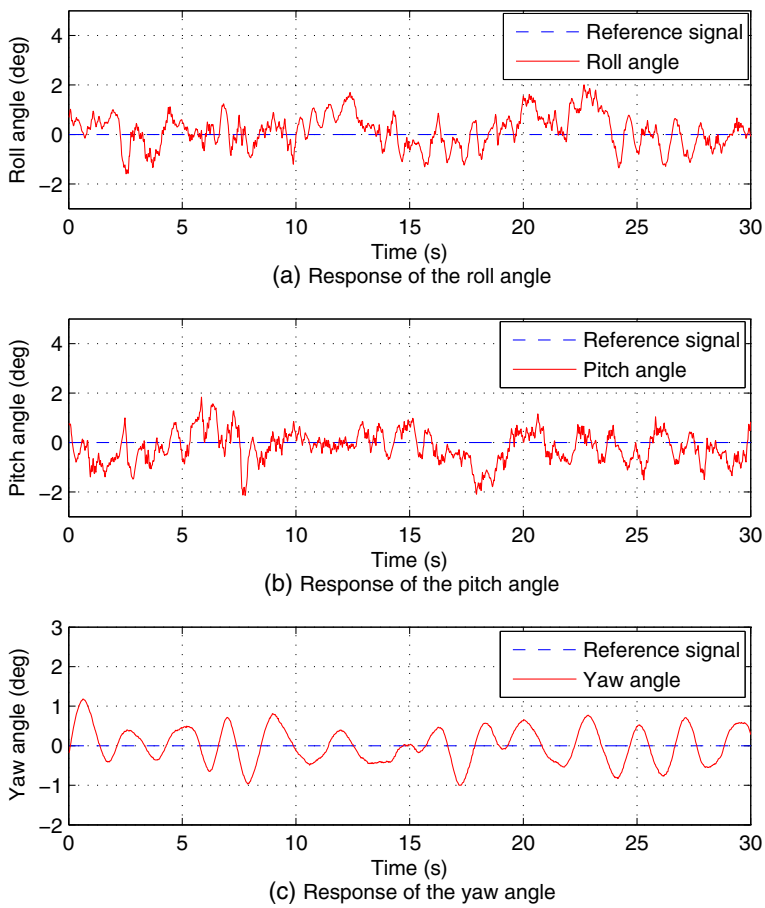

Fig. 5 Free flight hovering with the PD control method

$4\mu_\gamma(\mu_{x(0)} + \mu_c/\mu_x)^2/\varepsilon^2$. However, in practical applications, g_{i1} and $g_{i2}(i = 1, 2, 3)$ can be tuned on-line. One can set them to some initial positive values satisfying $g_{i1} \geq \eta_{gi} g_{i2}(i = 1, 2, 3)$, where η_{gi} is a large positive constant and is chosen according to practical situation. Then, run the attitude closed-loop system. If the performances of the system are unsatisfactory, one can set g_{i1} and $g_{i2}(i = 1, 2, 3)$ to larger values until the desired attitude tracking performances are achieved.

5 Experimental Results

As depicted in Fig. 4, an avionic system hangs below the quadrotor helicopter to implement the designed robust controller. The attitude loop runs at 100 Hz, which is the update rate of the IMU data collection and fusion. An external Kalman filter (EKF) is used for navigation data fusion. A low-cost scheme is used to collect the horizontal velocities of the quadrotor. The velocity measurement is based on an optical mouse sensor-ADNS2610 with a proper lens system. The flight computer can obtain the horizontal velocity of the vehicle from the outputs of ADNS2610. The altitude of the vehicle is obtained by an ultrasonic ranger. The position loop is updated with a sampling time 40 ms. Values of helicopter parameters are shown as in Table 1. In this section, the TAQS will carry out three tasks in order to demonstrate the effectiveness of the robust tracking controller designed in the previous section.

5.1 Case1: Hovering Tests

Attitude control is of crucial importance for a quadrotor to implement the hover mission. The

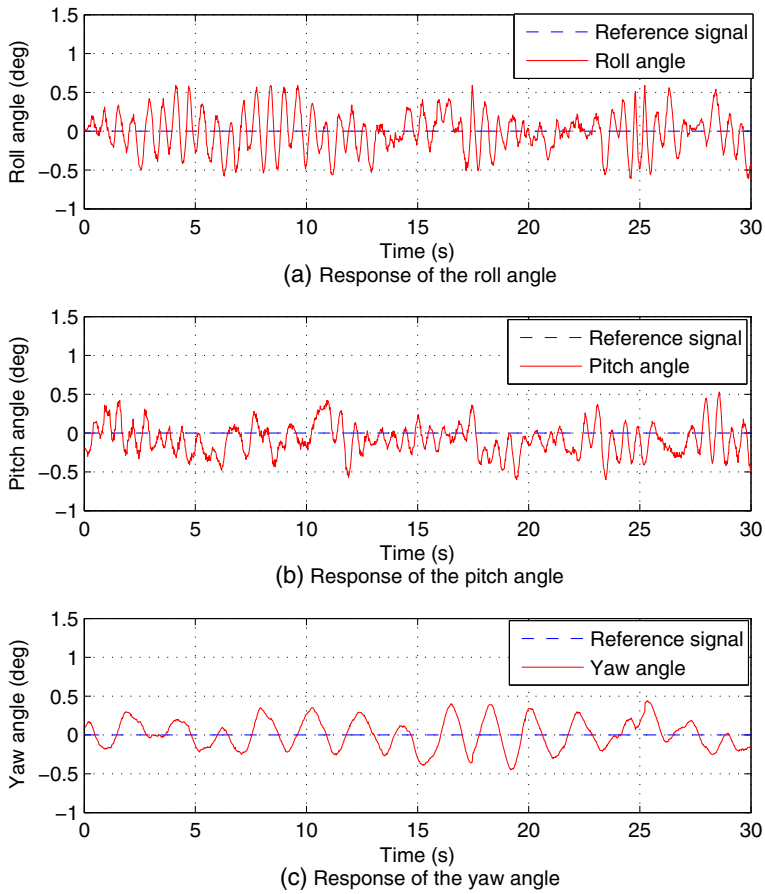

Fig. 6 Free flight hovering with the robust tracking control method

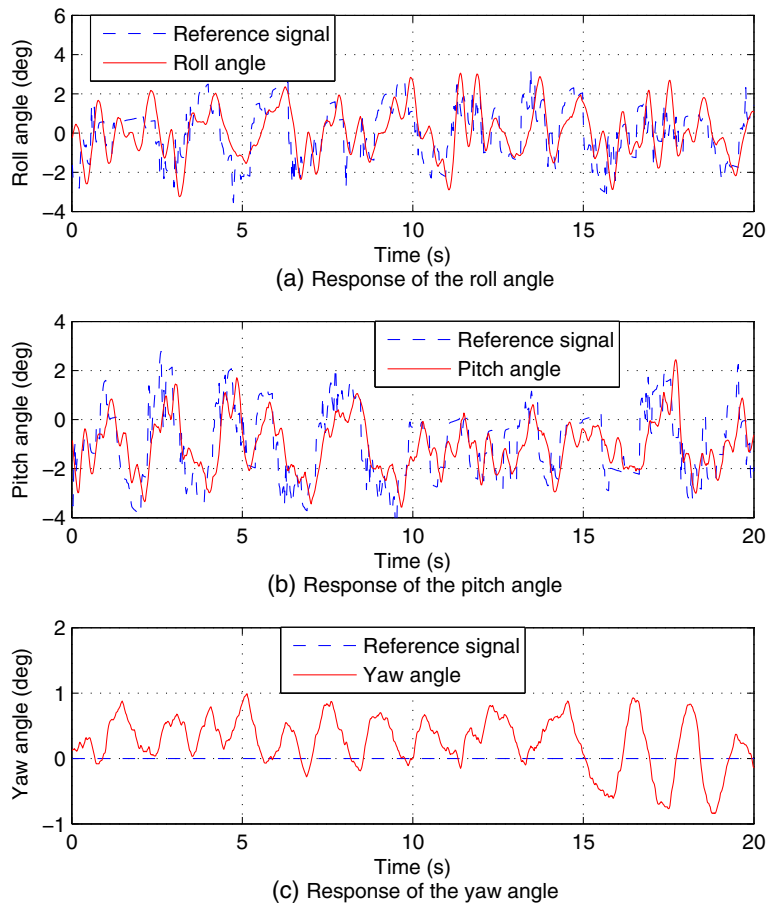

Fig. 7 Response of attitude angles in fixed position hovering

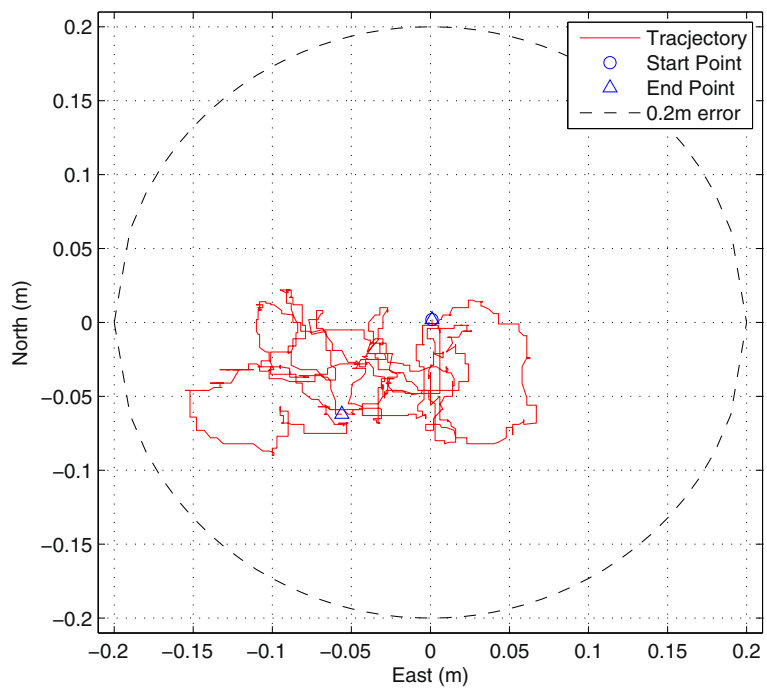

Fig. 8 Horizontal position of the TAQS in fixed position hovering test

parameters of the attitude controller are tuned in the hovering tests.

Firstly, the PD attitude controller parameters are tuned. The desired angles are set to be zeros. By trial and error, the parameters are set to be: $k_1^p = 6$, $k_1^d = 2$, $k_2^p = 6$, $k_2^d = 2$, $k_3^p = 4$, and $k_3^d = 2$ for good hovering performances. The attitude angle responses are depicted in Fig. 5.

Secondly, the robust compensator is added to improve the flight performances. After tuning the robust compensator parameters on-line monotonously, they are selected as: $g_{11} = 4$, $g_{12} = 20$, $g_{21} = 5$, $g_{22} = 20$, $g_{31} = 8$, and $g_{32} = 30$. The corresponding responses are presented in Fig. 6. From Fig. 5, one can see that the steady-state errors of the roll and pitch angles are achieved with amplitudes of ± 2 deg with the PD controller, whereas the robust attitude controller achieves steady-state errors of ± 0.6 deg as shown in Fig. 6. The robust compensating technique improves the hovering performances.

Thirdly, the parameters of position controller are tuned in fixed position hovering test for the TAQS. The prescribed four references and their derivatives $i_d^{(k)} = 0 (i = x, y, z, \psi; k = 0, 1, 2)$ are chosen. In this scenario, the desired roll and pitch angles are generated by the position controller. The position feedback control laws (4) can be implemented in practical applications. However, in order to simplify the expressions, the following approximated position control inputs θ_d and φ_d are applied

$$\theta_d = -\arcsin sat_{1-c_{\text{sat}}} \left(\left(k_x^p (\xi_x - x_d)/g + k_x^d \left(\dot{\xi}_x - \dot{x}_d \right)/g \right) \right),$$

$$\varphi_d = \arcsin sat_{1-c_{\text{sat}}} \left(k_y^p \left(\xi_y - y_d \right)/g + k_y^d \left(\dot{\xi}_y - \dot{y}_d \right)/g \right).$$

The position controller parameters can be tuned in a similar way after the parameters of

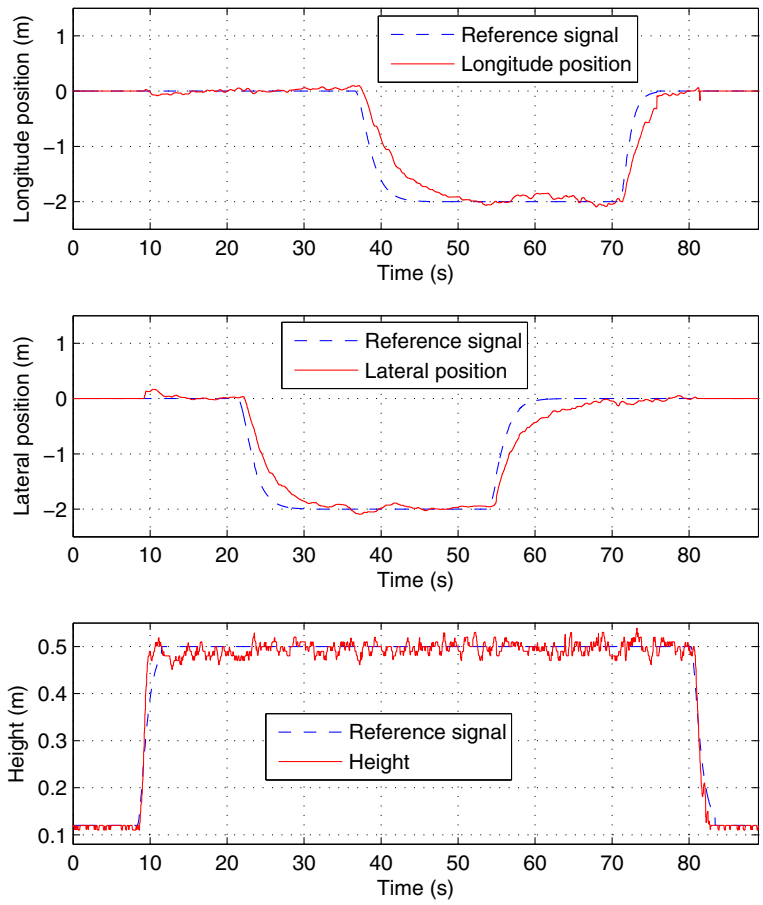

Fig. 9 Position responses in Case 2

Table 2 Parameters

Parameter	Value	Parameter	Value	Parameter	Value
x_{d0}	0	y_{d0}	0	z_{d0}	0.11
x_{d1}	−2	y_{d1}	−2	z_{d1}	0.5
x_{d2}	2	y_{d2}	2	z_{d2}	0.39
ω_{x1}	0.9	ω_{y1}	1	ω_{z1}	1.5
ω_{x2}	1.4	ω_{y2}	1	ω_{z2}	1.5
t_{x1}	37	t_{y1}	21	t_{z1}	8
t_{x2}	71	t_{y2}	54	t_{z2}	80

the attitude controller are determined. Set $k_x^p = 0.49$, $k_x^d = 4.9$, $k_y^p = 0.49$, $k_y^d = 4.9$, $k_z^p = 2.5$, and $k_z^d = 45$. The corresponding experimental results are depicted in Fig. 7. From this figure, one can see that the pitch and roll angles can follow the desired attitude references well, and the attitude tracking errors are within ±1 degree. The horizontal tracking performances of the closed-loop system are given in Fig. 8. It shows that the quadrotor can hover stably over a fixed-point within ±0.2 m.

5.2 Case 2: Trajectory Tracking Mission

In this experiment, the position control performances of the TAQS are evaluated. As shown in Fig. 1, the planner block of the ground station defines way-points and then generates trajectories for the quadrotor helicopter to follow. The helicopter is required to achieve the square trajectory tracking, which is defined by four way-points and corresponding responses of the three positions are depicted in Fig. 9. The task for the helicopter to carry out is to climb up to the position with a 0.5 m height from the ground and then follow the four sides of a square with the length of 2 m for each side. The distant from sonar sensor to the bottom of the quadrotor helicopter is 0.11 m, i.e., $\xi_z = 0.11$ m when the helicopter is sitting on the ground. The references $i_d (i = \psi, x, y, z)$ are chosen as $\psi_d(t) = 0$ and

$$i_d(t) = \begin{cases} i_{d0}, & t < t_{i1} \\ i_{d1} + i_{d2}(1 + \omega_{i1}(t - t_{i1}))e^{-\omega_{i1}(t-t_{i1})}, & t_{i1} \le t \le t_{i2} \\ i_{d0} - i_{d2}(1 + \omega_{i2}(t - t_{i2}))e^{-\omega_{i2}(t-t_{i2})}, & t > t_{i2} \end{cases}$$

where corresponding parameters are shown in Table 2. Figure 10 indicates that horizontal position errors during the flight can be controlled within ±0.2 m.

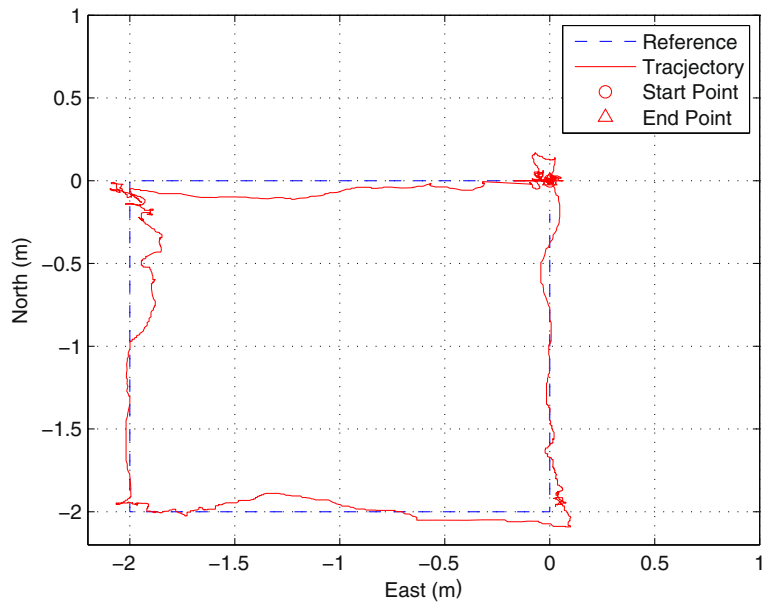

Fig. 10 Horizontal position of the TAQS in Case 2

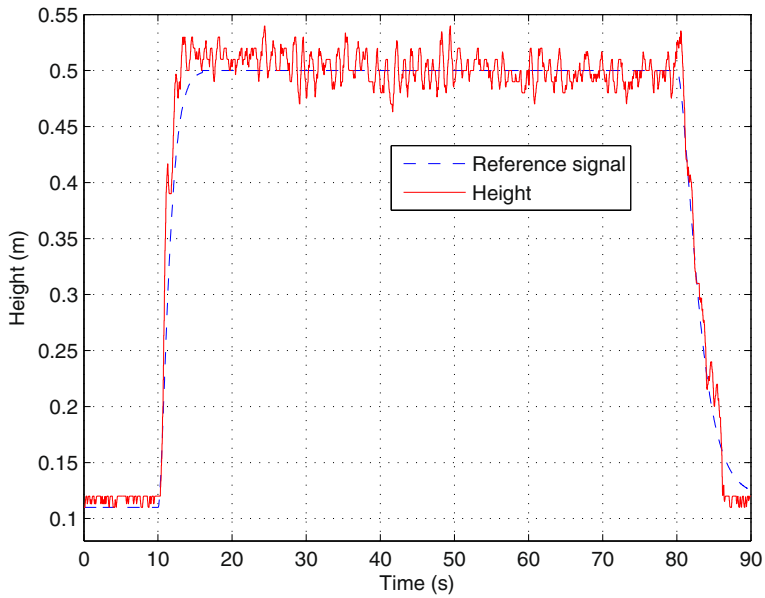

Fig. 11 Altitude response in Case 3

5.3 Case 3: Automatic Take-off and Landing Mission

Experimental results of automatic take-off and landing are depicted in Fig. 11. In this case, the TAQS is required to climb up to a position with a 0.5 m height, hover, and then land on the ground. In the landing part, when $z_d(t)$ is less than 0.2 m, all of the four rotors will stop rotating and the helicopter will land on the ground directly. $i_d^{(k)}(i = x, y, \psi; k = 0, 1, 2)$ are set to be 0. The desired reference for the height channel is given as

$$z_d(t) = \begin{cases} 0.11, & t < 10 \\ 0.5 - 0.39(1 + 1.2(t-10))e^{-1.2(t-10)}, & 10 \le t \le 80 \\ 0.11 + 0.39(1 + 0.6(t-80))e^{-0.6(t-80)}, & t > 80. \end{cases}$$

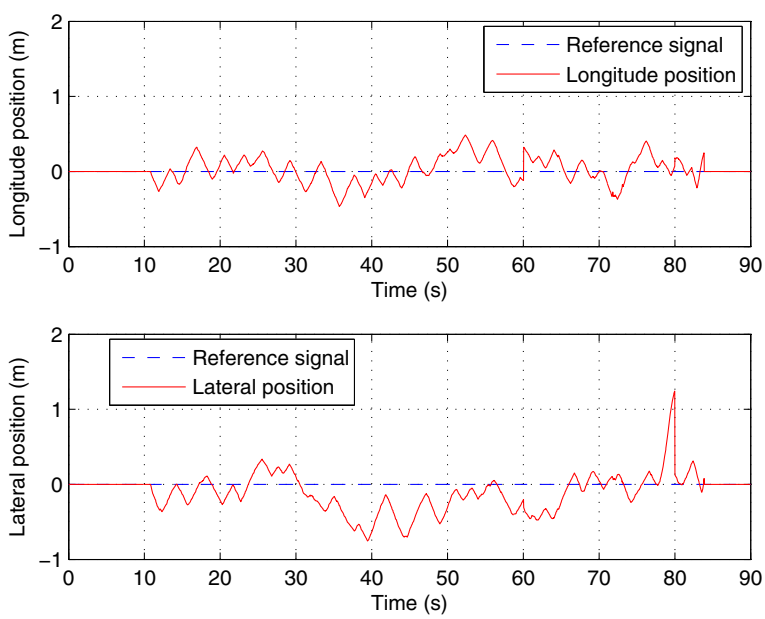

Fig. 12 Responses of the longitude and lateral position in Case 3

Figure 11 shows that the helicopter can follow the vertical references well. The corresponding responses in the longitude and lateral channels are depicted in Fig. 12. The tracking error of altitude channel is within ± 0.04 m.

6 Conclusions

A robust controller was proposed based on the time-scale separation approach to achieve the automatic take-off, hovering, trajectory tracking, and landing missions for a quadrotor helicopter. The designed controller consists of a position controller and an attitude controller. The position controller generates the desired pitch and roll angles based on the tracking errors of the longitudinal and lateral positions and is applied to follow the height reference for the vertical position. Based on the robust compensation technique, the attitude controller is designed to achieve the desired tracking of the attitude angles. It was proven that attitude tracking errors are proven to ultimately converge to the given neighborhoods of the origin. Experimental results on the quadrotor demonstrated the effectiveness of the proposed robust control method.

Acknowledgements This work was supported by National Nature Science Foundation of China under the Grants 61203071 and 61174067, as well as Tsinghua National Laboratory for Information Science and Technology (TNList) Basic Research Foundation.

References

1. Alexis, K., Nikolakopoulos, G., Tzes, A.: Switching model predictive attitude control for a quadrotor helicopter subject to atmospheric disturbances. Control Eng. Pract. **19**(10), 1195–1207 (2011)
2. Altug, E., Ostrowski, J.P., Taylor, C.J.: Control of a quadrotor helicopter using dual camera visual feedback. Int. J. Robot. Res. **24**(5), 329–341 (2005)
3. Castillo, P., Dzul, A., Lozano, R.: Real-time stabilization and tracking of a four-rotor mini rotorcraft. IEEE Trans. Control Syst. Tech. **12**(4), 510–516 (2004)
4. Marconi, l., Naldi, R.: Robust full degree-of-freedom tracking control of a helicopter. Automatica **43**(11), 1909–1920 (2007)
5. Xu, R., Ozguner, U.: Sliding mode control of a class of underactuated systems. Automatica **44**(1), 233–241 (2008)
6. Zuo, Z.: Trajectory tracking control design with command-filtered compensation for a quadrotor. IET Control Theory Applic. **4**(11), 2343–2355 (2010)
7. Tayebi, A., McGilvray, S.: Attitude stabilization of a VTOL quadrotor aircraft. IEEE Trans. Control Syst. Tech. **14**(3), 562–571 (2006)
8. Raffo, G.V., Ortega, M.G., Rubio, F.R.: An integral predictive/nonlinear H_∞ control structure for a quadrotor helicopter. Automatica **46**(1), 29–39 (2010)
9. Das, A., Subbarao, K., Lewis, F.: Dynamic inversion with zero-dynamics stabilization for quadrotor control. IET Control Theory Applic. **3**(3), 303–314 (2009)
10. Bertrand, S., Guenard, N., Hamel, T., Piet-Lahanier, H., Eck, L.: A hierarchical controller for miniature VTOL UAVs: design and stability analysis using singular perturbation theory. Control Eng. Pract. **19**(10), 1099–1108 (2011)
11. Hoffmann, G.M., Huang, H., Waslander, S.L., Tomlin, C.J.: Precision flight control for a multi-vehicle quadrotor helicopter testbed. Control Eng. Pract. **19**(9), 1023–1036 (2011)
12. Vilchis, J.C.A., Brogliato, B., Dzul, A., Lozano, R.: Nonlinear modelling and control of helicopters. Automatica **45**(10), 1583–1596 (2003)
13. Peng, K., Cai, G., Chen, B.M., Dong, M., Lum, K.Y., Lee, T.H.: Design and implementation of an autonomous flight control law for a UAV helicopter. Automatica **39**(9), 2333–2338 (2009)
14. Yu, Y., Zhong, Y.: Robust attitude control of a 3DOF helicopter with multi-operation points. J. Syst. Sci. Complex. **22**(2), 207–219 (2009)
15. Zheng, B., Zhong, Y.: Robust attitude regulation of a 3-DOF helicopter benckmark: theory and experiments. IEEE Trans. Ind. Electron. **58**(2), 660–670 (2011)
16. Liu, H., Lu, G., Zhong, Y.: Robust LQR attitude control of a 3-DOF lab helicopter for aggressive maneuvers. IEEE Trans. Ind. Electron. (2013, Available through early access)
17. Raptis, I.A., Valavanis, K.P., Moreno, W.A.: A novel nonlinear backstepping controller design for helicopters using the rotation matrix. IEEE Trans. Control Syst. Tech. **19**(2), 465–473 (2011)
18. Sira-Ramirez, H., Castro-Linarez, R., Liceaga-Castro, E.: A Liouvillian systems approach for the trajectory planning-based control of helicopter models. Int. J. Robust Nonlinear Control **10**(4), 301–320 (2000)
19. Zhong, Y.: Robust output tracking control of SISO plants with multiple operating points and with parametric and unstructured uncertainties. Int. J. Control **75**(4), 219–241 (2002)